Molecular Biology of the Cell
Vol. 8, 825–841, May 1997

Isolation and Molecular Characterization of mRNA Transport Mutants in *Schizosaccharomyces pombe*

Abul Kalam Azad, Tokio Tani, Naruhisa Shiki, Satomi Tsuneyoshi, Seiichi Urushiyama, and Yasumi Ohshima*

Department of Biology, Faculty of Science, Kyushu University, Higashi-Ku, Fukuoka 812–81, Japan

Submitted September 9, 1996; Accepted January 31, 1997
Monitoring Editor: Elizabeth Blackburn

Nucleocytoplasmic transport of mRNA is essential for eukaryotic gene expression. However, how mRNA is exported from the nucleus is mostly unknown. To elucidate the mechanisms of mRNA transport, we took a genetic approach to identify genes, the products of which play a role in that process. From about 1000 temperature-sensitive (ts^- or cs^-) mutants, we identified five ts^- mutants that are defective in poly(A)$^+$ RNA transport by using in situ hybridization with an oligo(dT)$_{50}$ as a probe. These mutants accumulate poly(A)$^+$ RNA in the nuclei when shifted to a nonpermissive temperature. All five mutations are tightly linked to the ts^- growth defects, are recessive, and fall into four different groups designated as *ptr 1-4* (poly(A)$^+$ RNA transport). Interestingly, each group of mutants has a differential localization pattern of poly(A)$^+$ RNA in the nuclei at the nonpermissive temperature, suggesting that they have defects at different steps of the mRNA transport pathway. Localization of a nucleoplasmin-green fluorescent protein fusion suggests that *ptr2* and *ptr3* have defects also in nuclear protein import. Among the isolated mutants, only *ptr2* showed a defect in pre-mRNA splicing. We cloned the *ptr2*$^+$ and *ptr3*$^+$ genes and found that they encode *Schizosaccharomyces pombe* homologues of the mammalian RCC1, a guanine nucleotide exchange factor for Ran/TC4, and the ubiquitin-activating enzyme E1 involved in ubiquitin conjugation, respectively. The *ptr3*$^+$ gene is essential for cell viability, and Ptr3p tagged with green fluorescent protein was localized in both the nucleus and the cytoplasm. This is the first report suggesting that the ubiquitin system plays a role in mRNA export.

INTRODUCTION

Eukaryotic cells are highly compartmentalized and movement of macromolecules between the compartments is an essential process for cellular functions. mRNA is one of such moving molecules, being exported out of the nucleus to the cytoplasm unidirectionally. Although the process of mRNA transport is an important control step in the eukaryotic gene expression, the molecular mechanism involved is not well understood.

The mRNA export seems to be a highly selective process and requires *cis*-acting signals (reviewed in Nigg *et al.*, 1991; Riedel and Fasold, 1992). The formation of functional mature mRNA is a prerequisite for transport in eukaryotes. mRNAs are transported to the cytoplasm after completion of the various processing events following transcription, such as 5′ capping, 3′ poly(A) addition, pre-mRNA splicing, and nucleotide modification. The structures formed in these steps of mRNA processing may work as signals for nucleocytoplasmic trafficking of mRNA. Based on an elegant series of microinjection experiments, it has been shown that the monomethyl cap structure might constitute such an export signal (Hamm and Mattaj, 1990). In addition, there is evidence of a linkage between 3′ end formation and the export of mRNA (Eckner *et al.*, 1991; Huang and Carmichael, 1996).

Export of mRNA from the nucleus seems to be an energy requiring and carrier mediated process (Moffet and Webb, 1981; French *et al.*, 1987; Schröder *et al.*, 1989). Experiments using microinjection into *Xenopus*

* Corresponding author.

oocytes showed that the export of various classes of RNA is, at least in part, mediated by class specific rather than common factors (Jarmolowski *et al.*, 1994). Therefore, RNA-protein interaction plays an important role in mRNA export. Recently, one of the most abundant nuclear RNA-binding proteins, hnRNP A1, was shown to shuttle between the nucleus and the cytoplasm (Piñol-Roma and Dreyfuss, 1991, 1992). A nuclear export signal was identified in that protein (Michael *et al.*, 1995), and these workers suggested that shuttling proteins like hnRNP A1 may serve as a carrier in RNA export to the cytoplasm. Similarly, Rev protein encoded by human immunodeficiency virus was reported to shuttle between the nucleus and the cytoplasm. This protein contains a similar nuclear export signal in its activation domain, suggesting that it also functions as an export carrier (Fischer *et al.*, 1995).

Beside these biochemical approaches, other investigators used genetic approaches to identify factors involved in mRNA export in yeast. They screened collections of yeast ts^- mutants to identify mutants that accumulate $poly(A)^+$ RNA in the nucleus at the nonpermissive temperature. These screens yielded 17 *mtr* (mRNA transport) and 10 *rat* (ribonucleic acid trafficking) mutants in *Saccharomyces cerevisiae* (Amberg *et al.*, 1992; Kadowaki *et al.*, 1994a) and 1 *rae* (ribonucleic acid export) mutant in *Schizosaccharomyces pombe* (Brown *et al.*, 1995). Characterization of those mutants revealed several factors required for the export process of mRNA. These factors are classified into three groups based on their localization. The first group consists of nucleoplasmic factors with diverse functions in the nucleus. For example, *RAT1* is an essential gene encoding a protein with regions of homology to Sep1p. RAT1 is a nucleic acid binding protein with a 5′-3′ exonuclease and DNA strand transfer activity (Amberg *et al.*, 1992). MTR1/PRP20 is a homologue of mammalian RCC1 and *S. pombe* Pim1p (Kadowaki *et al.*, 1993). RCC1 is a guanine nucleotide exchange factor for Ran/TC4 which is a small GTPase of the Ras superfamily. CNR1 and CNR2 were identified as a *S. cerevisiae* homologue of Ran/TC4 (Kadowaki *et al.*, 1993). MTR2 has a weak homology with a protein mbeA implicated in plasmid DNA transfer in *Escherichia coli* (Kadowaki *et al.*, 1994b). MTR13/NPL3 is thought to be involved in the bidirectional transport of macromolecules and contains RNA recognition motifs (Singleton *et al.*, 1995; Bossie *et al.*, 1992). Factors localized in the cytoplasm belong to the second group. The best known factor in this group is RNA1 (Shiokawa and Pogo, 1974). Recently, RNA1 was found to be a homologue of RanGAP1, a GTPase activator for Ran/TC4 (Bischoff *et al.*, 1995). The Rae1p in *S. pombe* also belongs to this group. The third group consists of a nucleoporin (nuclear pore complex protein) family. Several nucleoporins that play a role in nucleocytoplasmic transport of mRNA have been identified, including RAT2 (Heath *et al.*, 1995), RAT3/NUP133 (Li *et al.*, 1995), RAT7/NUP159 (Gorsch *et al.*, 1995), and several other nucleoporins (reviewed in Schneiter *et al.*, 1995).

Table 1. Yeast strains

Strain	Genotype	Source
HM123	*h⁻leu1-32*	M. Yanagida
SU32-5A	*h⁺ade6-M216*	This study
SU59-1D	*h⁻leu1-32*	This study
SU23-17B	*h⁺his2 leu1-32 ura4*	This study
975	*h⁺*	M. Yanagida
972	*h⁻*	M. Yanagida
A60	*h⁻leu1-32 ptr1-1*	This study
S2	*h⁻leu1-32 ptr1-2*	This study
S22	*h⁻leu1-32 ptr2-1*	This study
S13	*h⁻leu1-32 ptr3-1*	This study
T305	*h⁻leu1-32 ptr4-1*	This study
UDP6	*h⁺/h⁻ura4D18/ura4-D18 leu1-32/leu1-32 ade6-M216/ade6-M210*	This study

It is likely that many more factors involved in mRNA transport remain to be identified. Actually, most of the *mtr*, *rat* and *rae* genes described above have only one allele, suggesting that mutagenesis of the genes involved in mRNA transport is not yet saturated. To elucidate the mechanism of mRNA transport, we have isolated and characterized mutants defective in mRNA export in *S. pombe*, which is thought to be a good model organism of higher eukaryotes. Here, we report the identification of five mutations belonging to four complementation groups named *ptr 1–4* ($poly(A)^+$ RNA transport) and cloning of the $ptr2^+$ and $ptr3^+$ genes.

MATERIALS AND METHODS

Strains, Media, and Culture

The yeast strains used in this study are listed in Table 1. *S. pombe* were cultured using standard methods (Guthrie and Fink, 1991). Mutant or wild-type cells were routinely grown in a rich medium such as YPD. *E. coli* XL1-blue used for cosmid recovery was grown in LB (0.5% yeast extract, 1% tryptone, 0.5% NaCl, 0.1% glucose, pH 7.5; 1.5% agar was added for plates).

Mutagenesis

The wild-type strain $972h^-$ and HM123 (h^- *leu1–32*) was mutagenized with ethyl methanesulfonate (EMS) according to the method described by Vijayraghavan *et al.* (1989). Cells growing in a stationary phase were suspended at a density of $\sim 10^8$ cells/ml in 0.1 M sodium phosphate buffer (pH 7.0). The cells were then treated with 1.8–2.3% EMS at 30°C for 1 h. This treatment resulted in 10–20% cell survival. The suspension was neutralized by adding 5% sodium thiosulfate followed by dilution in distilled water and then plated on YPD plates for growth at 26°C for ts^- mutants, or at 32°C for cs^- mutants, for several days. After colonies appeared on plates, a replica of colonies was taken on YPD plates containing phloxin B, a dye that stains dead cells and facilitates the identification of ts^-

mutants. Replica plates were then kept at a nonpermissive temperature of 37°C (ts^-) or 22°C (cs^-).

Fluorescent In Situ Hybridization

Each ts^- mutant was grown in YE medium (0.5% yeast extract and 3% dextrose) at 26°C and shifted to 37°C for the indicated time. A cs^- mutant was grown at 32°C and shifted to 22°C for 6 h. The cells were then subjected to in situ hybridization as described (Tani *et al.*, 1995). Fixation of cells was done with freshly prepared 4% formaldehyde in 0.1 M Sörensen phosphate buffer (pH 6.0) for 1 h at room temperature. Cells were washed three times with PEM (100 mM PIPES, pH 6.9, 0.1 mM $MgCl_2$, 1 mM EGTA) containing 0.3 M glycine and then treated with 1 mg/ml of Novozyme 234 (Novo Nordisk, Bagsvaerd, Denmark) and Zymolyase 100T (Seikagaku Kogyo, Tokyo, Japan) in PEMS (PEM + 1.2 M sorbitol) for 10 to 15 min at 37°C. Spheroplasted cells were gently washed with cold PEMS and were put into the wells of Teflon-faced multiwell slides (Polyscience, Warrington, PA) coated with poly-L-lysine (M_r 150,000–300,000, Sigma Chemical, St. Louis, MO). After 20–30 min, nonadhered cells were removed by aspiration and dehydrated for 5 min each through a graded series of ethanol (70/90/100%). The slides were dried completely to avoid condensation and incubated in prehybridization buffer containing 4× SSC, 5× Denhardt's solution, and 1 mg/ml of tRNA at room temperature for 30 min. Hybridization was carried out with the same buffer containing 1 ng/μl of biotin- or digoxigenin-labeled oligo$(dT)_{50\text{-mer}}$ for 12 to 16 h at 37°C in a humidified chamber. Oligo(dT) was end labeled with a biotin-16-dUTP using a terminal transferase (Boehringer Mannheim, Indianapolis, IN) according to the manufacturer's instructions. Following hybridization, cells were washed four times in 4× SSC at 37°C (10 min/wash) and briefly rinsed with 4× SSC/0.1% Triton X-100. Cells were incubated with 4× SSC/1% bovine serum albumin containing fluorescein isothiocyanate (FITC)-avidin for 30 min at room temperature. Unbound FITC-avidin was washed out four times in 4× SSC and twice in 4× SSC/0.1% Triton X-100 at room temperature for 10 min each. The cells were counterstained with 1 μg/ml of 4',6-diamino-2-phenylindole (DAPI), mounted with a mounting medium [90% glycerol, 10% phosphate-buffered saline (PBS), 0.1% *p*-phenylenediamine], and examined under a Zeiss Axioplan microscope.

For triple staining, hybridized cells were washed as described above and then incubated with Texas Red-avidin at a dilution of 1:50 in 4× SSC/1% bovine serum albumin for 30 to 40 min at room temperature. Cells were washed with 4× SSC and 4× SSC/0.1% Triton X-100 as described above. After a brief incubation with PBS-1% bovine serum albumin/0.1% sodium azide/0.5% cold water fish skin gelatin (BAG), the cells were incubated with the D77 primary antibody at room temperature for 1 h in a humidified chamber. The cells were then washed three times with PBS for 10 min each and incubated with an affinity-purified fluorescein-conjugated goat anti-mouse IgG antibody at a dilution of 1:50 in PBS-BAG for 1 h at room temperature. After three washings with PBS, the cells were counterstained with DAPI as described above. The cells were finally examined under a confocal laser scanning microscope (LSM 410, Carl Zeiss, Thornwood, NY) equipped with a 100×, 1.3 aperature oil immersion lens, an argon ion laser to excite FITC fluorescence, a helium/neon laser to excite Texas Red fluorescence, and a UV laser for DAPI fluorescence.

A series of control experiments described below demonstrated the specificity of the in situ hybridization assay used here. First, the addition of a 500-fold molar excess of unlabeled oligo$(dT)_{50}$ in the hybridization buffer greatly diminished the nuclear signal (Figure 1C), showing the specificity of the oligo(dT) probe. Second, pretreatment of the cells with RNase T2 (adenosine-specific ribonuclease) before hybridization abolished the signal, possibly by destroying poly(A) sequences responsible for annealing with the probe (Figure 1E). This result also confirmed that the probe was hybridized specifically with poly(A)$^+$ RNA. In addition, when mutant cells were shifted to 37°C in the presence of 1,10-phenanthroline, which is a RNA polymerase inhibitor in yeast (Santiago *et al.*, 1986), the cells did not show nuclear signals (Figure 1G). These results clearly demonstrate that the assay used here indeed detected the accumulation of poly(A)$^+$ RNA in the nuclei.

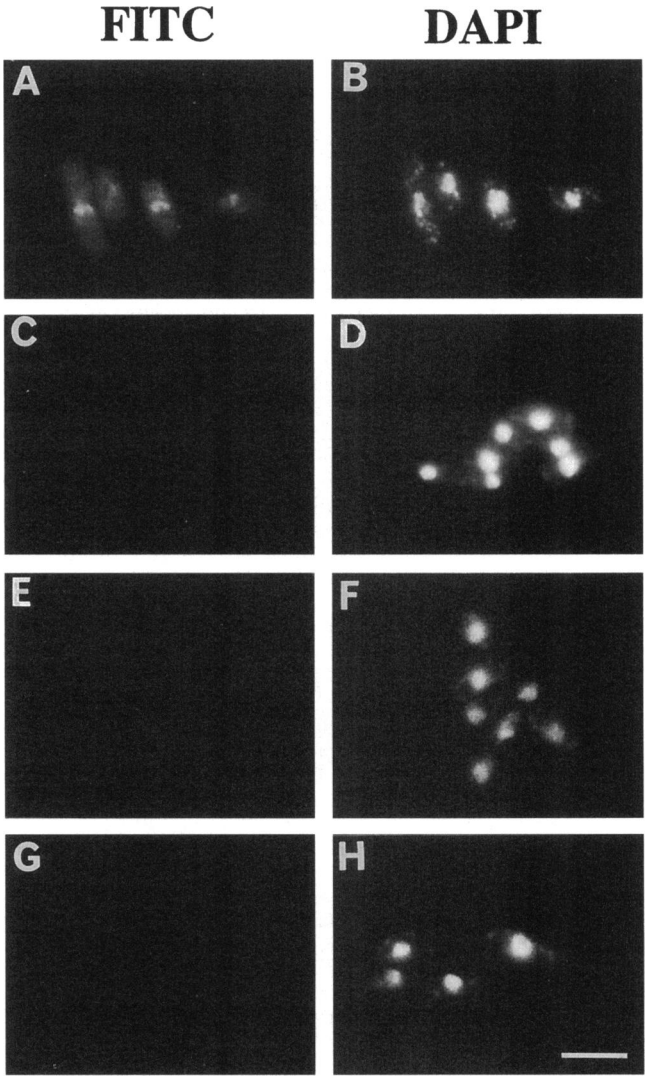

Figure 1. The in situ hybridization assay detects poly(A)$^+$ RNA specifically. The *ptr1–1* (A60) cells grown at 26°C were shifted to 37°C for 4 h and then subjected to in situ hybridization with the biotin-labeled oligo(dT) probe. Left and right columns show the poly(A)$^+$ RNA visualized using FITC (A, C, E, and G) and DNA stained with DAPI (B, D, F, and H), respectively. (A) Hybridization was done under the normal conditions described in MATERIALS AND METHODS. *ptr1* accumulates poly(A)$^+$ RNA in the nuclei. (C) Hybridization was performed in the presence of 500-fold molar excess of unlabeled oligo(dT). No hybridized signals were observed. (E) Cells were treated with 600 units/ml of RNase T2 at 37°C for 2 h before hybridization. Pretreatment with RNase T2 abolished the hybridized signals. (G) Addition of 300 μg/ml of 1,10-phenanthroline to the culture before shifting to 37°C resulted in no hybridization signal. Bar, 10 μm.

Genetic Analysis

All of the mutants that accumulated poly(A)$^+$ RNA in the nuclei at the nonpermissive temperature were backcrossed three times with

wild-type strains. Mating was usually done on a SPA plate. Diploid strains were constructed on an MM plate and maintained on a YE plate. Genetic manipulations of yeast cells, including strain construction, sporulation, random spore analysis, tetrad dissection, and heterozygous diploid analyses were performed according to the standard procedures as described (Guthrie and Fink, 1991).

Analysis of Nuclear Protein Import in ptr Mutants

To analyze nuclear protein import, we constructed a plasmid containing a chimeric DNA encoding a fusion of *Xenopus laevis* nucleoplasmin with green fluorescent protein (GFP; Chalfie *et al.*, 1994) in pREP3 (Maundrell, 1993) with an *nmt* promoter. The GFP-nucleoplasmin fusion protein was reported to be localized in the nucleus in *S. cerevisiae* (Lim *et al.*, 1995). The GFP-nucleoplasmin cDNA fragment was obtained by cutting the plasmid pCHR5ST (a gift from K. Khono, Nara Institute of Science and Technology, Japan, a S65T version of pAGN1 described by Lim *et al.*, 1995) with *Not*I and *Hin*dIII and was inserted into a *Bal*I site of pREP3. This plasmid was then introduced into the wild-type yeast strain HM123 and each of the *ptr* mutants. For protein import assay, cells were incubated at 26°C and grown to early log phase in MM medium without thiamine. Each culture was then either maintained at 26°C or shifted to 37°C for 12 h. Cells were examined for GFP fluorescence signal in a Zeiss Axioplan fluorescence microscope with a channel for FITC. Photographs were taken with the exposure time of 40–50 s.

Isolation and Analysis of RNA

To prepare total RNA, cells were usually grown to mid-log phase at 26°C. For Northern blot analysis of mutant strains, cells were shifted to 37°C for 2 h before harvesting. Total RNA was extracted from the cells by disruption with glass beads followed by phenol/chloroform/isoamyl alcohol treatment (Nischt *et al.*, 1986). Poly(A)$^+$ mRNA was isolated from total RNA by using an oligo(dT)-cellulose affinity chromatography as described (Sambrook *et al.*, 1989). For Northern blot analysis, total RNA or poly(A)$^+$ RNA was fractionated on a 1% agarose gel containing formaldehyde and transferred to a nylon membrane (Gene screen plus, New England Nuclear, Boston, MA) with 6× SSC. RNA was then fixed to the membrane by UV cross-linking. Filters were prehybridized for several hours at 42°C in 6× SSC/5× Denhardt's solution/0.1%SDS/100 μg/ml salmon sperm DNA/1 mM EDTA/50 mM sodium phosphate. Hybridization was carried out overnight at 42°C with the same buffer containing ^{32}P-labeled oligonucleotide probes complementary to the transcription factor IID (TFIID) pre-mRNA. The filter was washed once with 6× SSC at room temperature, twice with 6× SSC at 42°C, followed by washing at 42°C and at 55°C with 2× SSC/0.1%SDS for 10 min. The blot was exposed to a Fuji imaging plate and analyzed by a Bioimaging Analyzer BAS1000 (Fuji Photo Film Co., Kanagawa, Japan). To prepare the probes for Northern blot analysis, oligonucleotides complementary to the first intron (5′-GAAATCTCGTGACATGGTAG-3′) and the third exon (5′GAGCTTGGAGTCATCCTCGG -3′) of the TFIID pre-mRNA were 5′ end labeled using [γ-^{32}P]ATP (ICN Pharmaceuticals, Costa Mesa, CA) and T4 polynucleotide kinase.

Cloning and Sequencing

The *ptr*$^+$ genes were cloned by complementation of ts$^-$ growth phenotypes of the mutant strains with a genomic library constructed in a cosmid vector pSS10. Transformation was done using the lithium acetate method as described (Okazaki *et al.*, 1990). Leu$^+$ transformants at 37°C were examined using the instability test to distinguish rescued transformants from phenotypic revertants. Cosmid DNAs were recovered using *E. coli* XL1-blue and retested for their complementing ability for ts phenotypes. After several steps of subcloning into pSP1 (Cottarel *et al.*, 1993), the smallest fragment with rescue activity was identified. To determine the nucleotide sequence, nested deletions were prepared by the treatment of the genes cloned in the Bluescript KS$^+$ II with exonuclease III/mung-bean nuclease. Both strands of each gene were sequenced using an automatic DNA sequencer (ABI 373A DNA sequencer) and a Taq dye terminator cycle sequencing kit (Perkins Elmer, Foster City, CA).

A mutation site in the *ptr3–1* gene was localized within the *Hin*dIII-*Apa*I fragment (Figure 5) by using a gap repair method (Guthrie and Fink, 1991). This region was amplified from the *ptr3–1* gene by a polymerase chain reaction (PCR). Primers used for PCR were 5′-GCTGCTGACAGCCGTGGTC-3′ and 5′-AGGAATTAACCGGCTCTC-3′. The 2.6-kb PCR product was cloned into the pGEM-T cloning vector (Promega, Madison, WI) and sequenced. For isolation of the *ptr3*$^+$ cDNA, reverse transcription of total RNA with an oligo(dT) primer was used. The reverse transcription reaction products were then amplified by PCR with the above primers and cloned into the pGEM-T vector and sequenced. To determine the precise 5′ end of the gene, 5′ RACE was done according to manufacturer's instructions (Life Technologies, Gaithersburg, MD).

Integration Mapping

Targeted integration was performed as described previously (Guthrie and Fink, 1991). The 5.8-kb *Sac*I-*Sac*I *ptr3*$^+$ fragment was ligated to the *Sac*I site of Bluescript KS+II and the *leu2*$^+$ marker was inserted at the *Sma*I site in the same vector. The resulting plasmid containing *ptr3*$^+$ and the *leu2* $^+$ gene was linearized with *Hin*dIII and transformed into wild-type strain SU59–1D. Transformants were isolated for leucine prototrophy at the permissive temperature. DNAs were isolated from stable integrants and integration of the plasmid into the authentic *ptr3* $^+$ locus was confirmed by Southern blotting analysis. The strain in which the plasmid had integrated into the authentic locus was mated with the *ptr3–1* strain. Tetrads were dissected and haploid spores were analyzed for segregation pattern of temperature sensitivity and leucine auxotrophy.

Disruption of the ptr3$^+$ *Gene*

To disrupt the *ptr3*$^+$ gene, we replaced the *Hin*dIII-*Apa*I fragment in the *ptr3*$^+$ open reading frame (Figure 7) with the *S. pombe ura4*$^+$ gene. The fragment containing the *ptr3::ura4* disruption was introduced into the diploid strain UDP6. Stably integrated clones were isolated and replacement of *ura4* was confirmed by PCR analysis using primers from the *ura4* $^+$ gene and the *ptr3*$^+$ flanking sequence that was not replaced with *ura4* $^+$. The heterozygous diploids were sporulated at the permissive temperature and tetrads were dissected and analyzed.

Tagging of the ptr3$^+$ *Gene*

To construct a *ptr3* $^+$-GFP fusion gene, we first isolated a cDNA of GFP from the plasmid GFP-TT (a gift from Y. Jin and H.R. Horvitz, MIT, Boston, MA), which has the GFP cDNA in Tu 61 backbone, by cutting with *Age*I and *Apa*I. After treatment with the Klenow fragment of DNA polymerase I, the fragment was inserted into the *Mro*I site of the *ptr3* $^+$ gene (Figure 7). The resulting plasmid was then introduced into the *ptr3–1* strain. The transformants were examined by a fluorescent microscope to observe the expression of the Ptr3p-GFP fusion protein.

RESULTS

Screening of the Temperature-sensitive Mutants Defective in mRNA Transport

To identify mutants defective in mRNA transport, a bank of mutants temperature sensitive for growth was constructed by the treatment with EMS as described in

MATERIALS AND METHODS. The colonies which grew at 26°C (ts^-) or 32°C (cs^-) but failed to grow at 37°C (ts^-) or 22°C (cs^-) were saved for the mutant bank. The wild-type strains were able to grow at both temperatures. The concentration of EMS and incubation time required for mutagenesis were chosen to achieve ~20% survival after treatment. We used fluorescent in situ hybridization to screen for mutants that accumulated poly(A)$^+$ RNA in the nuclei at the nonpermissive temperature. Each mutant in the bank was first grown at the permissive temperature, shifted to the nonpermissive temperature for 2 to 6 h, and then subjected to in situ hybridization. Hybridization was done with a biotin-labeled or a digoxigenin-labeled oligo(dT)$_{50}$ probe, which anneals to the poly(A) tail of mRNA and pre-mRNA. Hybridized signals were detected with FITC-avidin or antidigoxigenin antibody conjugated to FITC. The cells were counterstained with DAPI that stains DNA and examined under an epifluorescence microscope. We screened a collection of about 1000 temperature-sensitive (~815 ts^- and ~185 cs^-) mutants and identified five ts^- mutants (A60, S2, S22, S13, and T305) that conditionally accumulated poly(A)$^+$ RNA in the nucleus.

Each mutant was then backcrossed three times with a wild-type strain. Analysis of several tetrads derived from each mutant showed 2:2 segregation of the ts^- and wild-type phenotypes, suggesting that the ts^- phenotype is due to a single mutation. To confirm that a single mutation is also responsible for the mRNA export defect, cells originating from each spore after the third backcross were subjected to in situ hybridization. In all cases, cosegregation of temperature sensitivity and nuclear accumulation of poly(A)$^+$ RNA was observed. In complementation analysis, diploids from A60 and S2 exhibited a ts^- phenotype, suggesting that these mutants belong to the same complementation group. The other three mutants fell into three distinct complementation groups. Thus, we named A60 (S2), S22, S13, and T305 as *ptr1*, *ptr2*, *ptr3*, and *ptr4* mutants, respectively. In situ hybridization with each heterozygous diploid showed no accumulation of poly(A)$^+$ RNA in the nuclei, suggesting that the mutations were recessive.

Figure 2 shows results of in situ hybridization with *ptr1-ptr4* or wild-type cells. In wild-type cells grown at either temperature (26°C or 37°C), poly(A)$^+$ RNA was distributed throughout the cells (Figure 2, A and C), indicating efficient transport of mRNA from the nucleus to the cytoplasm. At the permissive temperature, all of the mutants showed a uniform distribution of poly(A)$^+$ RNA throughout the cell (Figure 2, E, I, M, and Q), thereby reflecting that mRNA transport is not blocked in these mutants at this temperature. In contrast, *ptr1* shifted to the nonpermissive temperature for 2 h showed nuclear accumulation of poly(A)$^+$ RNA in 40–50% of the cells. The concomitant decrease of cytoplasmic mRNA in those cells suggested that mRNA transport was inhibited. When *ptr1* was shifted to the nonpermissive temperature for 4 h, the percentage of cells showing nuclear accumulation of poly(A)$^+$ RNA increased to 80–90% (Figure 2G). In *ptr2*, the nuclear poly(A)$^+$ RNA signals were observed in about 50% of the cells after 2 h at 37°C (Figure 2K). The percentage of cells with nuclear signals decreased (~10%) after 4 h at 37°C in *ptr2*. Both *ptr3* and *ptr4* mutants showed nuclear accumulation of poly(A)$^+$ RNA in 40–50% cells after 2 h at 37°C (Figure 2, O and S). There was no significant increase or decrease in the percentages of cells with nuclear signals when shifting time was extended to 4 h in these mutants. Interestingly, the nuclei with accumulated poly(A)$^+$ RNA were localized to corners in some of the *ptr4* cells (Figure 2S).

To determine whether the mRNA transport block was reversible or not, all four mutants were first shifted to the nonpermissive temperature for 2 h and then returned to the permissive temperature for 2 h before being subjected to in situ hybridization. The poly(A)$^+$ RNA was again found to be distributed throughout the cell, showing that these mutants are able to resume mRNA transport at the permissive temperature.

In addition, each mutant was incubated at 37°C to accumulate poly(A)$^+$ RNA in the nuclei and then was maintained at 37°C with 1,10-phenanthroline. Because intense nuclear signals persisted after this treatment, the accumulated poly(A)$^+$ RNA is sufficiently stable in the nuclei. Accumulation of poly(A)$^+$ RNA in the nuclei in all of the mutants was analyzed also at 15, 30, 60, and 90 min after the shift to the restrictive temperature. No significant accumulation of poly(A)$^+$ RNA was observed in all cases at least before 90 min after the shift.

Growth and viabilities of the wild-type and the mutants after shift to the restrictive temperature were examined (Figure 3). *ptr2* lost viability quickly, *ptr1* slowly, and *ptr3* and *ptr4* at an intermediate rate. The increase in the fraction of *ptr1* cells with nuclear poly(A)$^+$ RNA accumulation from 40 to -50% at 2 h to 80 to 90% at 4 h as described before, and the decrease in *ptr2* cells from about 50% at 2 h to about 10% at 4 h may be correlated with slow and rapid loss of viabilities in *ptr1* and *ptr2*, respectively. No gross morphological changes occurred in the mutants at 2 or 4 h after the shift except for *ptr3*, some cells of which became fattened at 4 h.

Localization of Poly(A)$^+$ RNA in the Nuclei of the Mutant Cells

To analyze localization of the poly(A)$^+$ RNA within the nuclei, triple staining was carried out using the oligo(dT)$_{50}$ probe, the D77 antibody that specifically

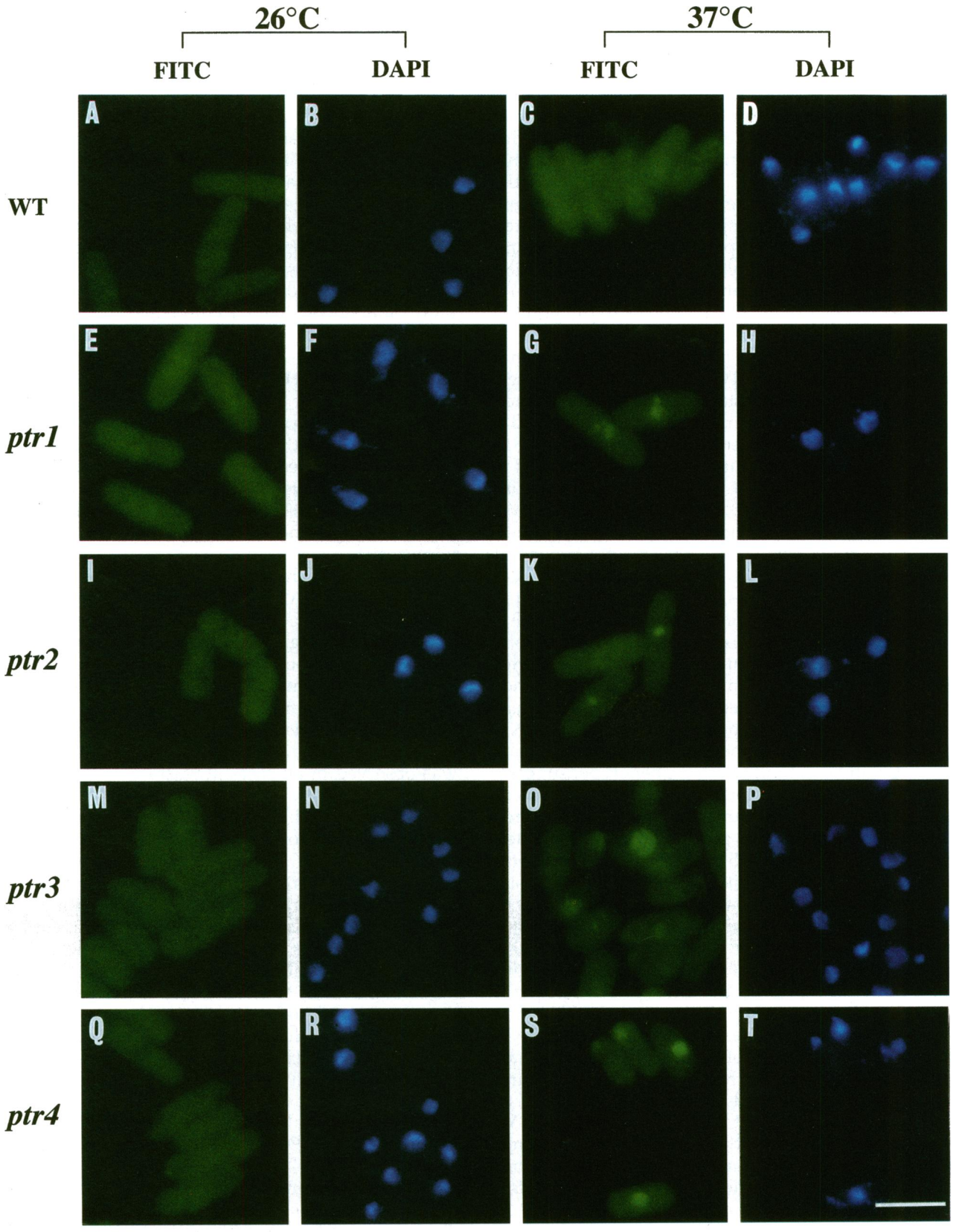
26°C
37°C
FITC
DAPI
FITC
DAPI
A
B
C
D
WT
E
F
G
H
ptr1
I
J
K
L
ptr2
M
N
O
P
ptr3
Q
R
S
T
ptr4

Figure 2.

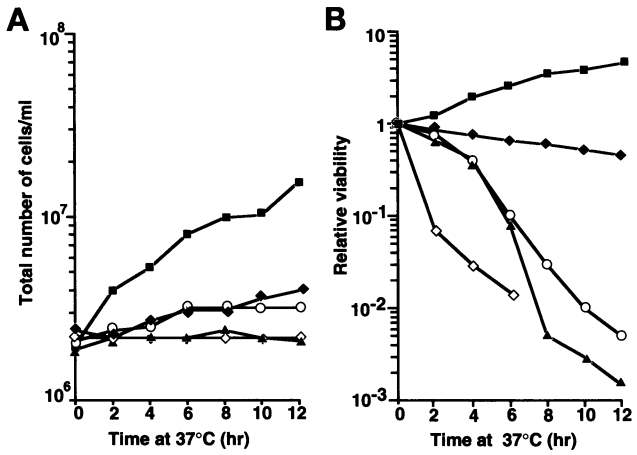

Figure 3. Growth characteristics of the *ptr* mutants at the nonpermissive temperature. The wild-type and the mutant strains were grown in YPD to a mid-log phase at the permissive temperature (26°C) and diluted into fresh media. They were then cultured at 37°C for the indicated times. Total numbers of the cells were determined using a hemacytometer (A). Relative viability of the cells was obtained from the number of colonies grown on YPD plates at 26°C for 3 days (B). The symbols represent the strains as follows: closed square, wild type; closed diamond, *ptr1–1*; open diamond, *ptr2*; closed triangle, *ptr3*; and open circle, *ptr4*.

recognizes a nucleolar protein, fibrillarin (Aris and Blobel, 1988; Tani *et al.*, 1995), and DAPI which stains DNA. In the wild-type strain, poly(A)$^+$ RNA was uniformly distributed throughout the cells at 26°C and 37°C (Figure 4, A and a). The D77 antibody stains the nucleolar region where fibrillarin is located, occupying about one-half of the nucleus (Figure 4, B and b). DAPI stains a chromatin-rich region that does not overlap with fibrillarin and occupies about the other half of the nucleus (Figure 4, C and c). Poly(A)$^+$ RNA, fibrillarin, and DAPI in the *ptr1-4* mutants cultured at the permissive temperature (26°C) showed distribution patterns similar to those seen in wild-type cells (Figure 4, H, L, P, and T). In contrast, when these mutants were shifted to the nonpermissive temperature (37°C), differential sublocalization patterns for poly(A)$^+$ RNA were observed. In *ptr1* incubated at 37°C for 4 h, accumulation of poly(A)$^+$ RNA was observed in two to three discrete spots (Figure 4, e). The merged image shows that mRNA did not accumulate either in the DNA region or in the fibrillarin region (Figure 4, h). The site of accumulation of poly(A)$^+$ RNA in this mutant seems to be outside of those two regions. On the other hand, poly(A)$^+$ RNA coincides with the D77 staining region in *ptr2*, giving an overlapping image in yellow in the merged picture at the nonpermissive temperature (Figure 4, l). The accumulated poly(A)$^+$ RNA is clearly separated from the chromatin-rich region. In the *ptr3* cells incubated at 37°C for 4 h, poly(A)$^+$ RNA was colocalized with the DNA stained by DAPI (Figure 4, p). The area occupied by accumulated poly(A)$^+$ RNA is somewhat larger than that of the chromatin-rich region. In this case poly(A)$^+$ RNA does not accumulate in the fibrillarin-rich region. In *ptr4* cells, the accumulation site of poly(A)$^+$ RNA mostly overlapped with the chromatin-rich region (Figure 4, t). Interestingly, not all *ptr4* cells at the nonpermissive temperature were stained with the D77 antibody. The *ptr4* cells that accumulated poly(A)$^+$ RNA did not show the D77 staining and vice versa (Figure 4, r and s). We examined 10–20 cells of the wild type and each of the mutant strains to correctly localize accumulation of the poly(A)$^+$ RNA in the nuclei.

Figure 2 (facing page). *ptr* mutants have defects in poly(A)$^+$ RNA transport at the nonpermissive temperature. Wild-type (A–D), *ptr1–1* (E–H), *ptr2* (I–L), *ptr3* (M–P), and *ptr4* (Q–T) cells were grown at 26°C and either maintained at 26°C (left two columns) or shifted to 37°C for 4 h in *ptr1–1*, 2 h in other strains (right two columns). The cells were fixed and analyzed by in situ hybridization with the biotin-labeled oligo(dT)$_{50}$ probe. Hybridized signals were detected by FITC-conjugated avidin. The FITC columns show the distribution of poly(A)$^+$ RNA in the respective cells. The DAPI columns show staining of DNA of the cells in the same field. FITC and DAPI photographs were taken with exposure times of 50–60 s and 5–10 s, respectively. WT, wild type. Bar, 10 μm.

Defects in Nuclear Protein Import in the ptr Mutants

To analyze whether *ptr* mutations cause defects in nuclear protein import or not, we examined the distribution of a GFP-nucleoplasmin fusion protein in the wild type and mutants. The cells expressing the fusion protein were either maintained at 26°C or shifted to 37°C for 12 h (Figure 5). At 26°C, nuclear accumulation of the fusion was shown in about 80% of the cells in wild type, *ptr1*, *ptr2*, and *ptr4* and in 40–50% cells in *ptr3*. These results indicate that the fusion protein is normally imported to the nucleus in wild type and in *ptr1*, *ptr2*, and *ptr4* at 26°C. It is probably the case also in *ptr3* since derepressed synthesis of the fusion protein in *ptr3* cells, which did not show nuclear accumulation of the fusion, seemed to be ineffective for an unknown reason. Since fluorescence of the GFP-nucleoplasmin synthesized at 37°C is much less than that synthesized at 23°C or 30°C (Lim *et al.*, 1995) and since the *ptr* mutants have defects in mRNA export at 37°C, most of the fluorescence observed at 37°C in the *ptr* mutants should represent that of the fusion protein synthesized before the temperature shift. This interpretation is further supported by the results that addition of thiolutin (2 μg/ml) or cycloheximide (10 μg/ml) just before the temperature shift did not significantly alter the fluorescent distribution or intensity. Therefore, uniform distribution of the fluorescence at 37°C in *ptr2* and *ptr3* suggests diffusion of the

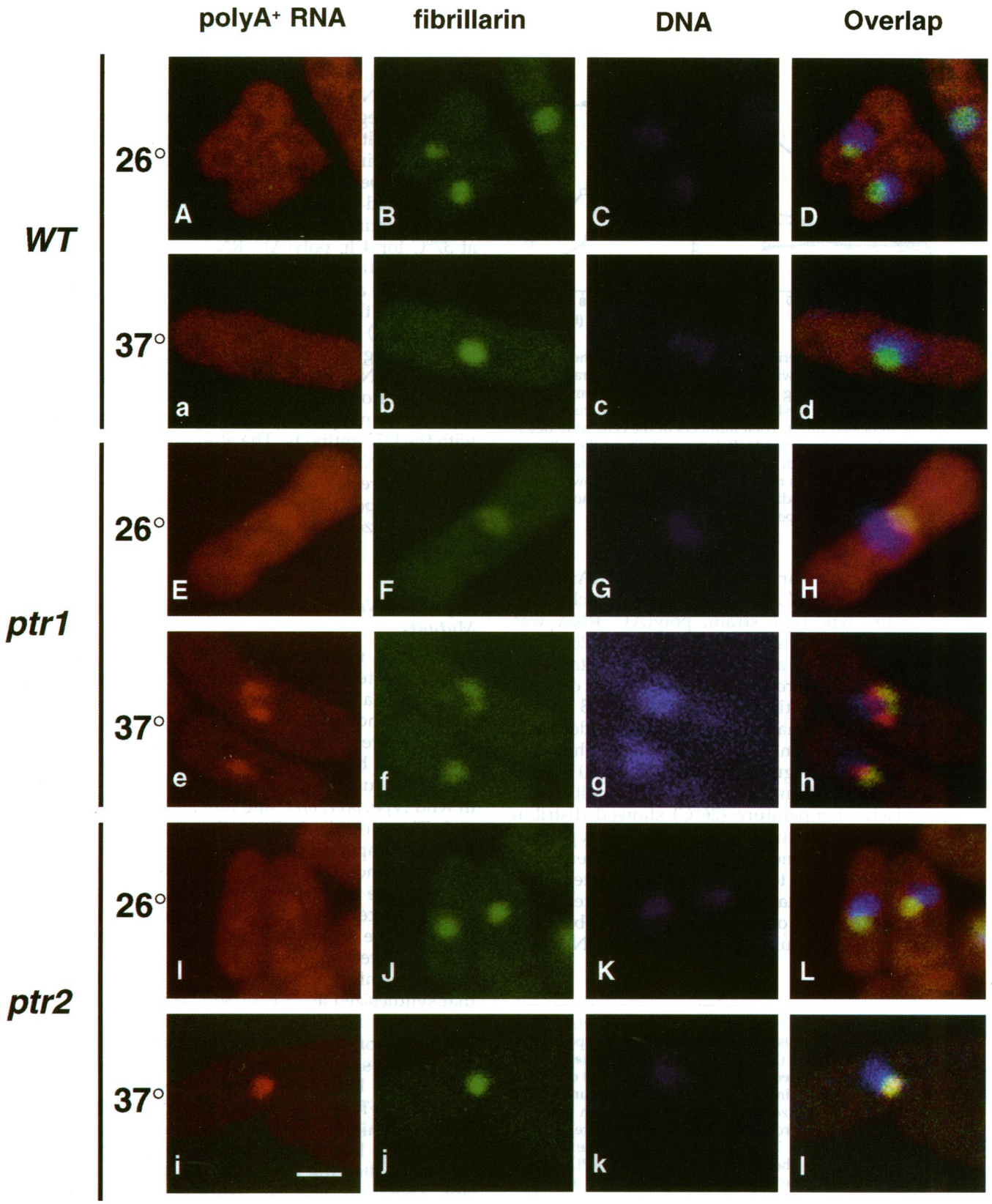
polyA+ RNA
fibrillarin
DNA
Overlap
WT
ptr1
ptr2
26°
37°
A
B
C
D
a
b
c
d
E
F
G
H
e
f
g
h
I
J
K
L
i
j
k
l

Figure 4.

GFP-nucleoplasmin from the nucleus into the cytoplasm and a block of its reimport at 37°C in these mutants. In contrast, nuclear accumulation of the fusion protein in *ptr1* and *ptr4* at 37°C suggests that these mutants do not have a defect in its import.

ptr 2 Has Defects in Pre-mRNA Splicing

It was reported that mutations in *MTR1/SRM1/PRP20* and *RNA1* caused defects in RNA processing as well as in RNA export (Kadowaki *et al.*, 1994a; Forrester *et al.*, 1992). To examine whether the *ptr* mutations affect pre-mRNA splicing at the nonpermissive temperature, total cellular RNA isolated from cells incubated at 26°C or cells after the shift to 37°C for 2 h was subjected to Northern blot analysis of TFIID mRNA. The oligonucleotide probes were used which were complementary to the first intron or third exon sequences of TFIID pre-mRNA. As shown in Figure 6, wild-type, *ptr1*, *ptr3*, and *ptr4* cells did not show accumulation of TFIID pre-mRNA at both permissive and nonpermissive temperatures. Also, the amounts of mature TFIID mRNA in the mutants described

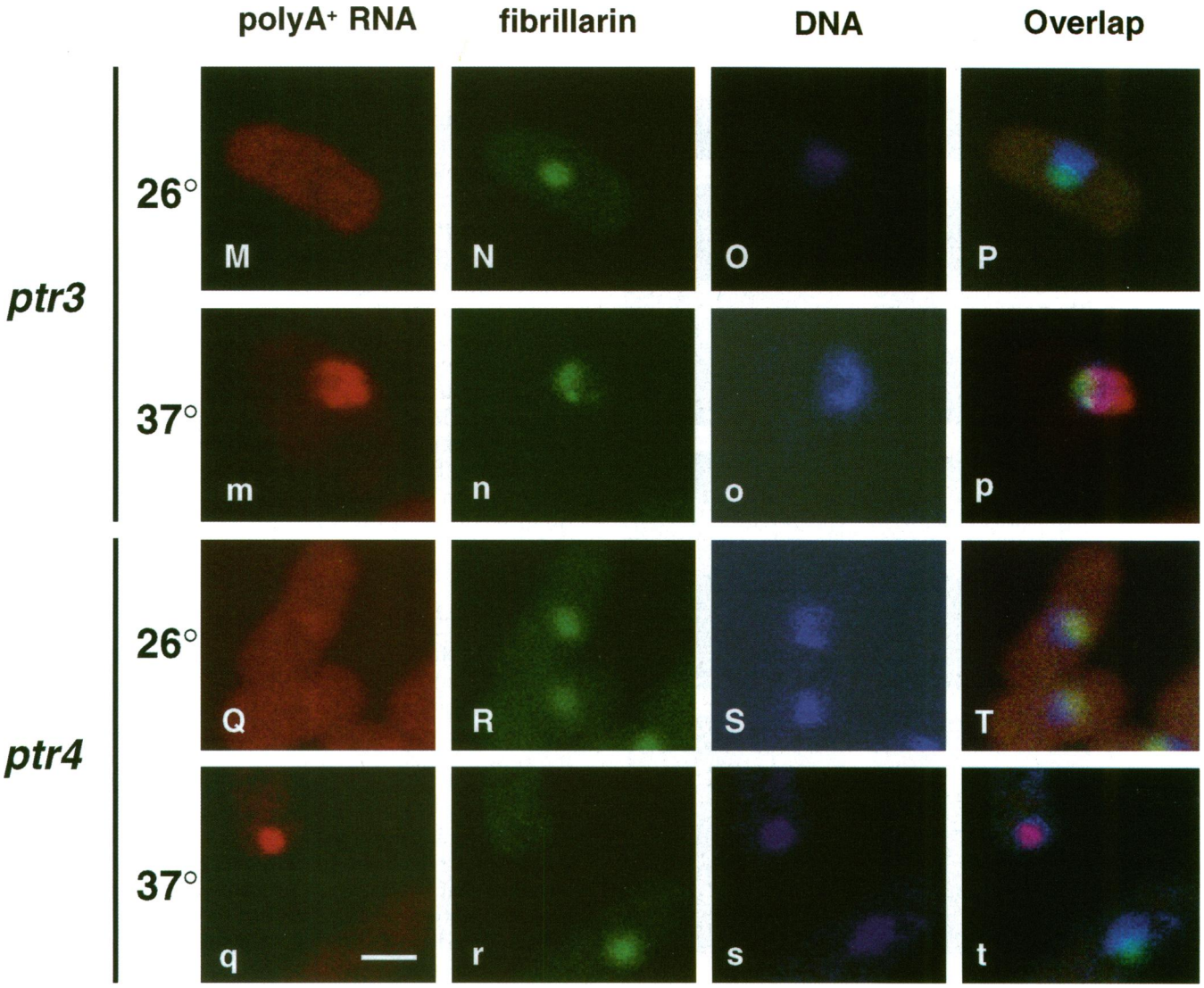

Figure 4 (cont). Localization of accumulated poly(A)$^+$ RNA in the nuclei. Wild-type and mutant cells were grown at 26°C and either maintained at 26°C (images in capital letters) or shifted to 37°C for 4 h (images with small letters), and then subjected to triple staining with the biotin-labeled oligo(dT) probe (poly(A)$^+$ RNA), D77 antibody (fibrillarin), and DAPI (DNA). Images were taken using a confocal laser scanning microscope equipped with an UV laser. In the merged images marked as "Overlap," red denotes poly(A)$^+$ RNA, green denotes fibrillarin, blue denotes DNA staining, yellow denotes colocalization of poly(A)$^+$ RNA and fibrillarin, and pink denotes colocalization of poly(A)$^+$ RNA and DNA. WT, wild type. Bars, 3.5 μm.

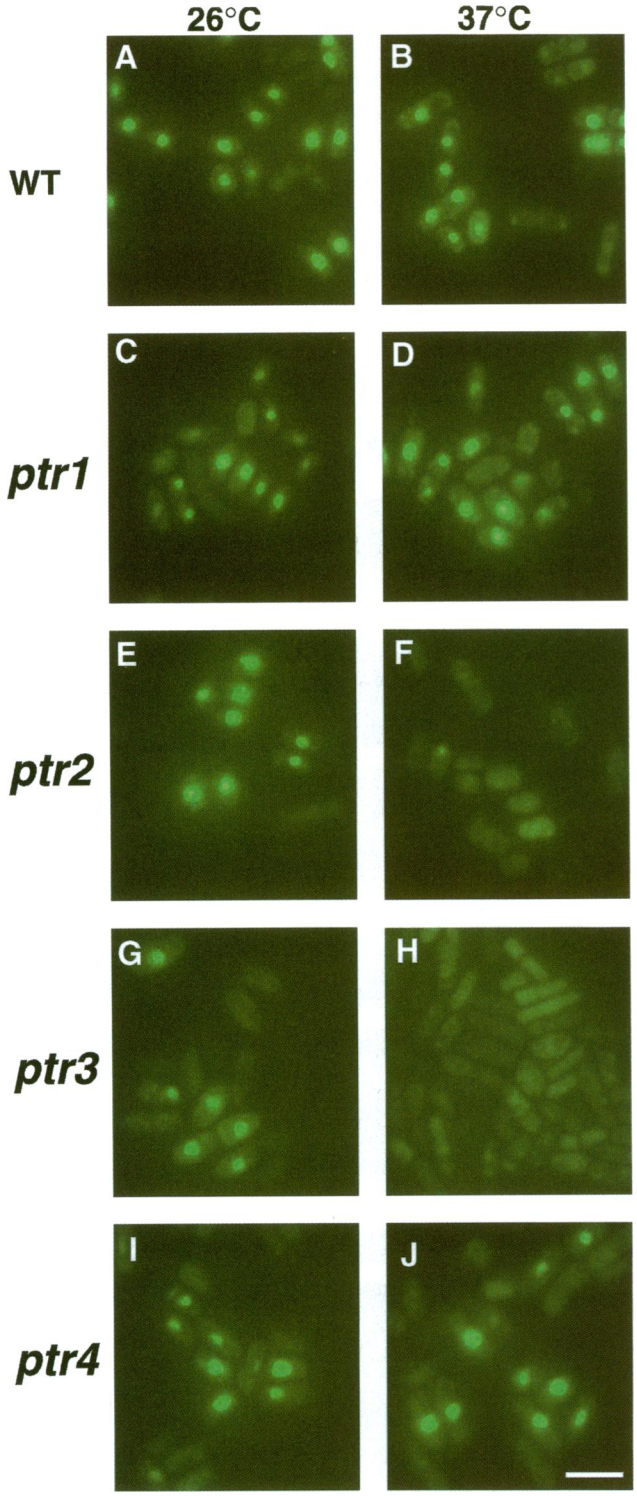

Figure 5. Nuclear protein import in *ptr* mutants. Wild type (A and B), *ptr1–1* (C and D), *ptr2* (E and F), *ptr3* (G and H), and *ptr4* (I and J) carrying a nucleoplasmin-GFP fusion gene under an *nmt* promoter were grown at 26°C and maintained at 26°C (left column) or shifted to 37°C for 12 h (right column). Nuclear protein import was analyzed by observation of the GFP-nucleoplasmin fusion protein as described in MATERIALS AND METHODS. WT, wild type. Bar, 10 μm.

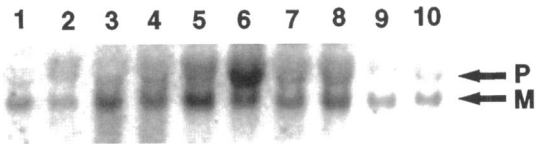

Figure 6. Pre-mRNA splicing in *ptr* mutants. Wild-type (lanes 1 and 2), *ptr1-1*(lanes 3 and 4), *ptr2* (lanes 5 and 6), *ptr3* (lanes 7 and 8), and *ptr4* (lanes 9 and 10) cells were grown at 26°C and either maintained at 26°C (lanes 1, 3, 5, 7, and 9) or shifted to 37°C for 2 h (lanes 2, 4, 6, 8, and 10). Total RNAs were then isolated from the cells and analyzed by Northern blot analysis with the TFIID probes. P and M indicate the positions of the precursor and mature TFIID mRNA, respectively.

above did not change after shifting to the nonpermissive temperature. In contrast, in *ptr2*, a precursor of TFIID mRNA was accumulated and the amount of mature mRNA decreased at the nonpermissive temperature (Figure 6, lane 6). These results suggest that pre-mRNA splicing is defective in the *ptr2* mutant, but not in the other three mutants.

Cloning of ptr2$^+$ and ptr3$^+$ Genes

To isolate the genes responsible for the defects in mRNA transport described above, we transformed the mutants with a *S. pombe* wild-type genomic library and isolated cosmid clones that complemented the temperature-sensitive growth defects of the *ptr2* and *ptr3* mutants. These cosmid clones could also rescue the defects in mRNA transport in *ptr2* and *ptr3*.

After several steps of subcloning, the activity complementing the *ptr2* mutation was detected in a 3.8-kb fragment in the cosmid. The partial nucleotide sequences of the regions essential for complementation showed that *ptr2*$^+$ was identical to *pim1*$^+$, which is a *S. pombe* homologue of the mammalian *RCC1* gene encoding a guanine nucleotide exchange factor for Ran/TC4. The results of the genetic mapping showed that the distance between *his2* and *ptr2* was 19.7 cM and that between *ptr2* and *cdc10* was 22.3 cM. These genetic distances are close to those between *pim1* and *his2* and between *pim1* and *cdc10*, respectively (Matsumoto and Beach, 1991), supporting that *ptr2* is allelic with *pim1*. The *pim1* mutation was initially identified as a ts$^-$ lethal allele that caused premature chromosome condensation and mitotic spindle formation (Matsumoto and Beach, 1991). Kadowaki *et al.* (1993) showed that both the mammalian tsBN2 mutant that has a mutation in the *RCC1* gene and *S. pombe pim1* accumulated poly(A)$^+$ RNA in the nuclei at the restrictive temperature.

ptr3$^+$ Encodes a Ubiquitin-activating Enzyme E1

Two cosmid clones complementing *ptr3* were isolated. Those cosmids were found to contain identical segments of genomic DNA. One of the cosmids,

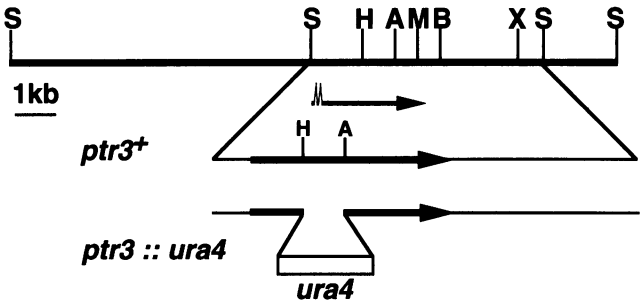

Figure 7. Restriction map of the DNA fragment that rescues the *ptr3* mutation. Arrow denotes an open reading frame encoding Ptr3p and the direction of transcription. The kinked lines represent introns. A, *Apa*I; B, *Bgl*II; H, *Hin*dIII; M, *Mro*I; S, *Sac*I; X, *Xho*I. Gene disruption strategy is shown. The *Hin*dIII-*Apa*I fragment was replaced with *ura4*$^+$ gene (open box) to obtain the *ptr3::ura4* null allele.

that contained an insert of ~34 kb, was selected for further study. This cosmid clone complements ts$^-$ growth defect and also the defect in poly(A)$^+$ RNA transport in *ptr3–1*. A restriction map of this cosmid is shown in Figure 7. Several restriction fragments were subcloned to identify a gene region. We found that a 5.8-kb *Sac*I fragment was sufficient for complementation of the ts$^-$ growth defect as well as the transport defect in *ptr3*. To exclude the possibility that the cloned gene is a multicopy suppressor for *ptr3*, we performed integration mapping as described in MATERIALS AND METHODS. Integration of the cloned gene linked with a *LEU2* marker into the authentic locus was confirmed by Southern blot analysis (data not shown). One of these stable integrants was crossed with the *ptr3–1* strain and several tetrads were dissected. All of the ts$^-$ spore progenies were found to be leucine auxotrophs and all ts$^+$ progenies leucine prototrophs, confirming that the cloned gene complementing the *ptr3* mutation is genetically linked to the *ptr3*$^+$ locus.

The nucleotide sequence of the 5.8-kb fragment containing the *ptr3*$^+$ gene was determined (Figure 8). An open reading frame of 3201 nucleotides was found, encoding a protein of 1012 amino acid residues with a predicted molecular mass of ~110 kDa. The size of the gene was consistent with the result of Northern blot analysis, which indicated that the *ptr3*$^+$ gene generates a mRNA of 3.4 kb in length (data not shown). To determine the precise 5′ end of the gene, we cloned the cDNA corresponding to the 5′ region of the *ptr3*$^+$ mRNA by using the 5′ RACE method and identified two introns in the 5′ region of the gene (Figure 8).

Comparison of the nucleotide sequence of the *ptr3*$^+$ gene with those in the European Molecular Biology Laboratory database using the BLAST program (Altschul *et al.*, 1990) showed that the *ptr3*$^+$ has a high homology (~59%) with the genes encoding a ubiquitin-activating enzyme E1 in *S. cerevisiae* and human (Zacksenhaus and Sheinin, 1990; McGrath *et al.*, 1991). Figure 9 shows the alignment of amino acid sequence of the Ptr3p with that of *S. cerevisiae* ubiquitin-activating enzyme E1. The E1 enzyme catalyzes the activation of ubiquitin, the first step common to all of the ubiquitin conjugation. The predicted amino acid sequence of the Ptr3p contains one glycine-rich motif (Gly–X–Gly–X–X–Gly) characteristic of a nucleotide-binding domain, which is highly conserved among wheat, *S. cerevisiae*, and human E1 enzymes (McGrath *et al.*, 1991; Zacksenhaus and Sheinin, 1990).

To identify a mutation site in the *ptr3–1* allele, a gap repair experiment was performed. A gap between *Hin*dIII and *Apa*I sites was made in the *ptr3*$^+$ gene and the resultant linear plasmid carrying the *leu*$^+$ marker was used to transform the *ptr3–1* mutant. All of the *leu*$^+$ transformants were temperature sensitive at 37°C, which means that a mutation is present within this region, confirming again that we have cloned the bona fide *ptr3*$^+$ gene. To exactly locate the mutation site in the *ptr3–1*, the region containing the mutation site was amplified by PCR and sequenced. Sequences of the several clones obtained from two independent PCR reactions revealed the presence of a single point mutation at nucleotide position 1892, which changes C to A (a replacement of amino acid threonine to lysine), in the gene.

ptr3$^+$ *Is an Essential Gene*

To determine whether the *ptr3*$^+$ gene is essential for growth of *S. pombe* cells, we disrupted one copy of the *ptr3*$^+$gene in a wild-type diploid strain by one-step gene replacement. We constructed a *ptr3::ura4* disrupted gene (Figure 7) and used it to transform a diploid strain lacking the *ura4* gene. A transformant with the correct integration was subjected to tetrad analysis. The tetrads analyzed never yielded more than two viable spores and none of these viable spores were able to grow on plates without uracil. Thus, the product of the *ptr3* gene is essential for growth.

Localization of Ptr3p

To determine the subcellular location of Ptr3p, we tagged Ptr3p with GFP as described in MATERIALS AND METHODS. The tagged *ptr3*$^+$ gene was capable of complementing temperature sensitivity of the *ptr3–1* strain, demonstrating that the fusion protein is functional. The transformants that contained the fusion protein were examined by a fluorescence microscope. We observed fluorescence throughout the cells (Figure 10A). This means that GFP-tagged *ptr3* protein is present in both the nucleus and the cytoplasm. A control plasmid encoding Ptr3p without a GFP tag did not give any fluorescence (Figure 10C). Uba1p, ubiquitin-activating enzyme E1 in *S. cerevisiae*, was also

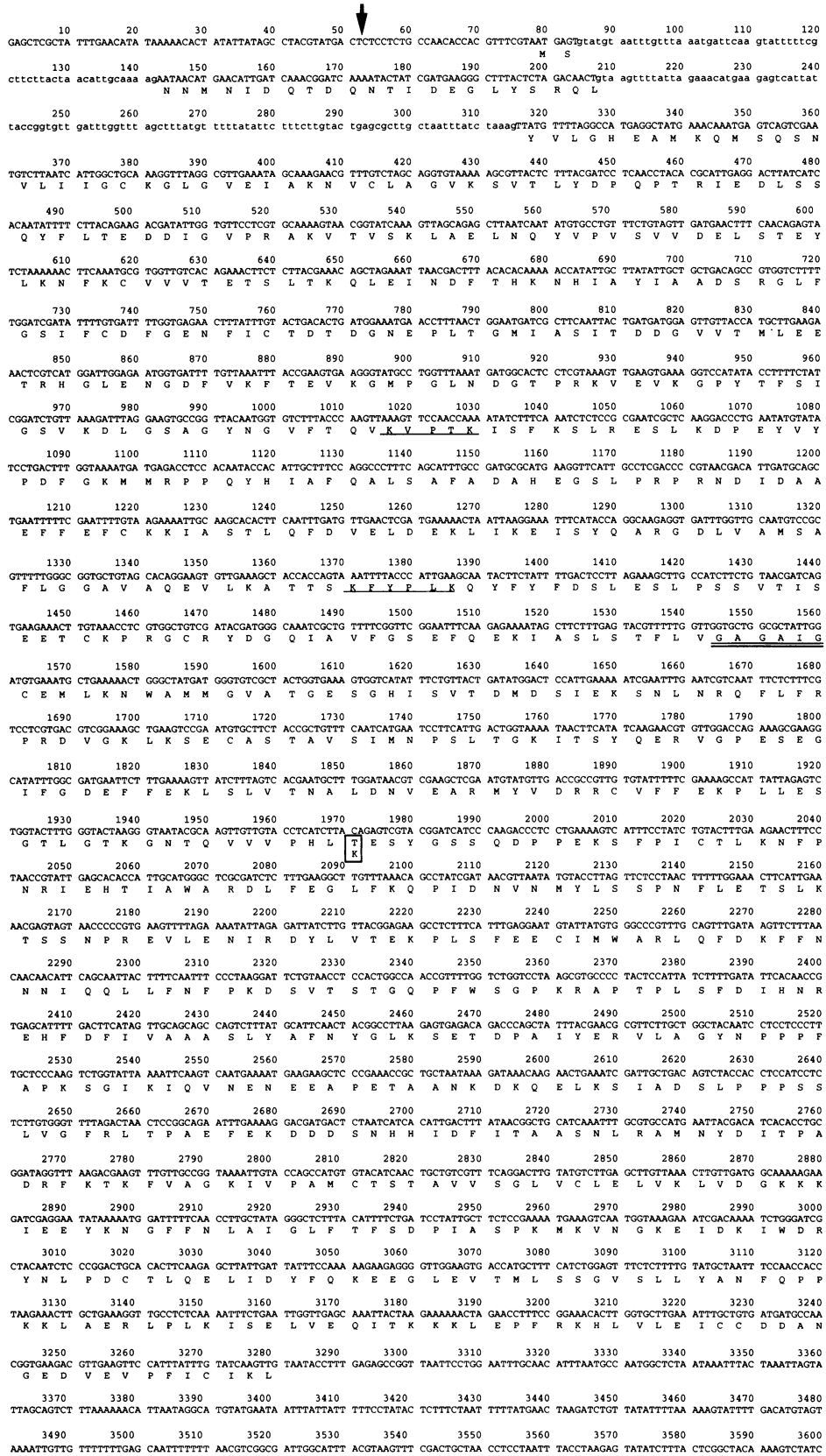

Figure 8. The nucleotide sequence of the *ptr3*$^{+}$ gene and the predicted amino acid sequence in a single-letter code. Nucleotide residues are numbered above the sequence. Intron sequences are shown by small letters. Arrow indicates a presumed initiation site for transcription. The two underlined sequences represent putative nuclear targeting signals. A motif characteristic of a nucleotide-binding domain is double underlined. The amino acid replacement found in *ptr3–1* is shown below the sequence and boxed. Position 1 is the *Sac*I site. The nucleotide sequence reported here is available in the DNA Data Bank of Japan, European Molecular Biology Laboratory, and GenBank databases under the accession number D87259.

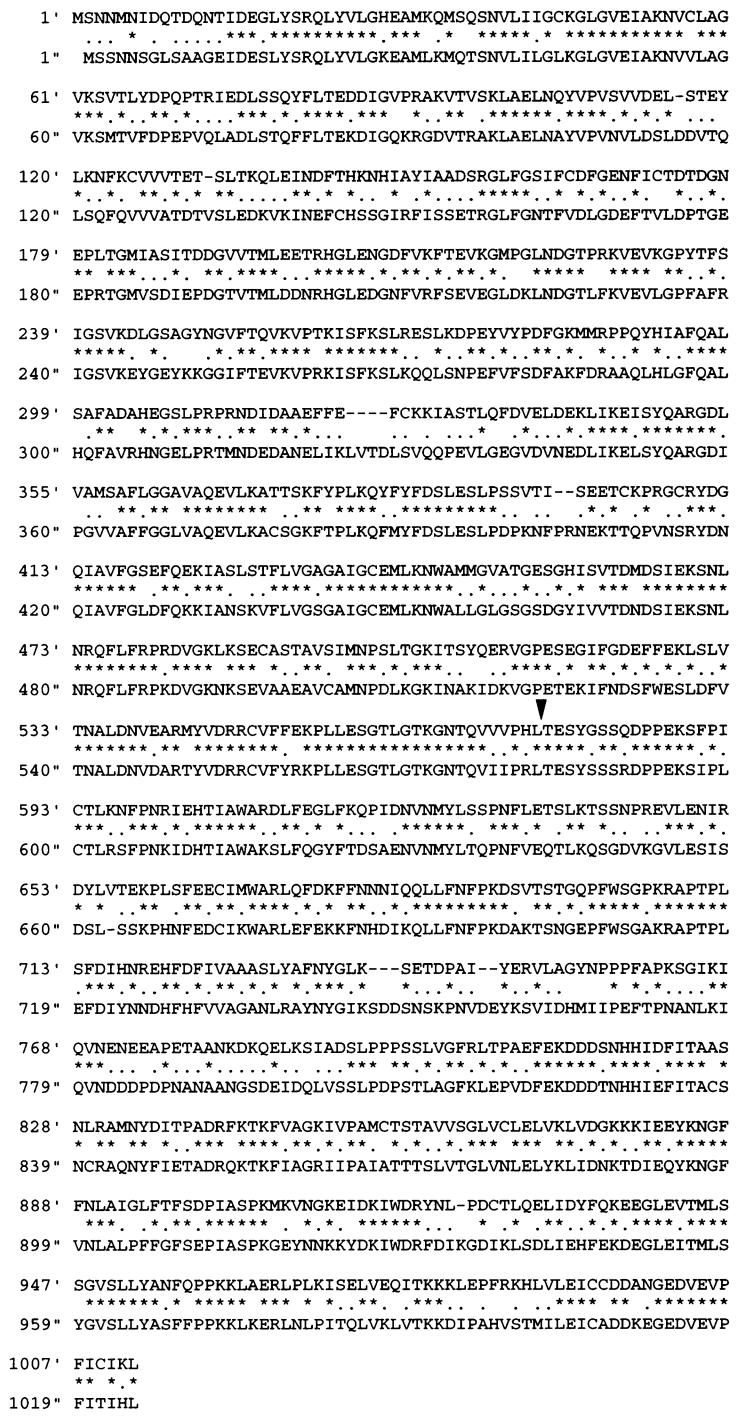

Figure 9. Comparison of the amino acid sequences between Ptr3p and ubiquitin-activating enzyme E1 in *S. cerevisiae*. The upper sequence represents the Ptr3p sequence and the lower one that of ubiquitin-activating enzyme E1 in *S. cerevisiae*. Identical and similar amino acids between the two proteins are shown by asterisks and dots, respectively. Arrowhead denotes the amino acid mutated in *ptr3–1*.

shown to be localized in both the nucleus and the cytoplasm (Dohmen *et al.*, 1995).

DISCUSSION

In *S. pombe*, one mutation named *rae1* that causes defects in poly(A)$^+$ RNA export was identified by the screening with in situ hybridization (Brown *et al.*, 1995). The *rae1*$^+$ gene encodes a protein of 352 amino acids with β-transducin/WD40 repeats. In the present study, we have isolated five other recessive mutants defective in nucleocytoplasmic transport of poly(A)$^+$ RNA at the nonpermissive temperature. Complementation analysis of these mutants showed that they

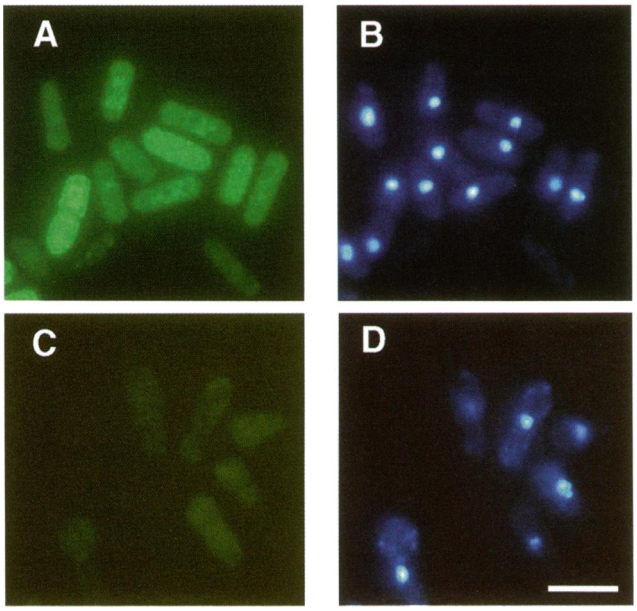

Figure 10. Intracellular localization of Ptr3p. *ptr3* cells bearing a *ptr3p/GFP* fusion gene or *ptr3* $^{+}$ gene were grown at 26°C and the GFP fluorescence was observed by FITC channel of a fluorescence microscope. (A) *ptr3* cells with the *ptr3p/GFP* gene. (B) Corresponding DAPI image of A. (C) *ptr3* cells carrying the *ptr3* $^{+}$gene. (D) DAPI image of cells in C. Photographs were taken with the exposure time of 30 s. Bar, 10 μm.

belong to four distinct groups named *ptr1-4*. Interestingly, we observed differential patterns of poly(A)$^{+}$ RNA localization in the nuclei at the nonpermissive temperature among the *ptr* mutants, suggesting that these mutants have defects at different steps of mRNA transport.

Nucleolar Accumulation of the Poly(A)$^{+}$ RNA in ptr1 and ptr2 Mutants

In *ptr1*, poly(A)$^{+}$ RNA accumulates in two to three foci in the nuclei at the nonpermissive temperature (Figures 2G and 4e). Nuclear accumulation of poly(A)$^{+}$ RNA in spots or foci are also observed in several *S. cerevisiae* mRNA transport mutants such as *mtr2* and *rat3* (Schneiter *et al.*, 1995). The foci containing the poly(A)$^{+}$ RNA in *S. pombe ptr1* did not overlap with either the DAPI-stained region or the fibrillarin-rich region of the nucleolus (Figure 4h). The nucleus of the wild-type yeast cells consists of two regions readily distinguished by an electron microscopic analysis. One region with electron-dense materials occupying about one-third or one-half of the nucleus has been referred to as the nucleolus and the other half with less electron-dense materials as the chromatin-enriched region. At the permissive temperature, fibrillarin is distributed throughout the nucleolar region in *ptr1* cells (Figure 4F) as in wild-type cells (Figure 4B). However, after shifting the cells to the nonpermissive temperature, the fibrillarin-rich region looked condensed and fragmented (Figure 4f), and simultaneously poly(A)$^{+}$ RNA was accumulated in the nucleolar region not stained either by the antifibrillarin antibody or by DAPI (Figure 4h). Thus, there are likely to be several distinct subnucleolar compartments in the yeast.

The *ptr2* mutant also accumulates the poly(A)$^{+}$ RNA in the nucleoli at the nonpermissive temperature. However, in the case of *ptr2*, the site of accumulation of poly(A)$^{+}$ RNA mostly coincides with the fibrillarin-rich region (Figure 4, i, j, and l). It has been reported that several mRNA transport mutants in *S. cerevisiae* accumulate poly(A)$^{+}$ RNA in the nucleoli at the nonpermissive temperature (Schneiter *et al.*, 1995). In addition, a severe heat shock blocks mRNA transport in *S. pombe* and results in the accumulation of bulk poly(A)$^{+}$ RNA in the nucleoli (Tani *et al.*, 1995). These observations led to the hypothesis that the yeast nucleolus may play a role in mRNA transport in addition to its role in rRNA synthesis and preribosome assembly (Schneiter *et al.*, 1995; Tani *et al.*, 1995). Predominant localization of poly(A)$^{+}$ RNA in the nucleoli in *ptr1* and *ptr2* at the nonpermissive temperature also supports the foregoing hypothesis, although we would need to exclude an alternate possibility that the yeast nucleolus functions as a deposit site for the mRNAs which are not exported to the cytoplasm.

ptr3 and ptr4 Accumulate Poly(A)$^{+}$ RNA in the DNA Region

In contrast to *ptr1* and *ptr2*, accumulation sites of poly(A)$^{+}$ RNA in the *ptr3* and *ptr4* mutants coincide with the chromatin-rich region (Figure 4, p and t), a result which suggests that these mutants may have defects in the early steps of the export pathway, such as those required for the release of mRNAs from the sites of transcription or processing.

Interestingly, *ptr4* shows a typical phenotype of *cut* (cell untimely torn) mutations (Hirano *et al.*, 1986). In the *cut* mutants, the coordinated mitosis is completely disrupted. Septation and cytokinesis in these mutants occur in the absence of nuclear division, resulting in the cleavage of the undivided nucleus. Cytokinesis without prior nuclear division leads to localization of the damaged nucleus at an extremity of the cell. More than 60% of the *ptr4* cells incubated at the nonpermissive temperature for 4 h showed the "*cut*" phenotype. Because the *ptr4* cells without the *cut* phenotype (i.e., the cells with the normal nuclei) also accumulated poly(A)$^{+}$ RNA in the nuclei (see Figure 2, S and T), the block of the poly(A)$^{+}$ RNA export in this mutant is not due to structural damages in the nucleus generated by uncoordinated cytokinesis. Rather it seems to be a direct consequence of the mutation.

Well-known mutations that show the *cut* phenotype include *top2* as well as the series of *cut* mutations. The *top2*$^+$ gene encodes DNA topoisomerase II, which catalyzes the concerted cleavage and rejoining of DNA strands (Uemura and Yanagida, 1984) and is involved in formation of the mitotic chromosome (Uemura and Yanagida, 1986) and the chromosome scaffold (Earnshaw *et al.*, 1985). On the other hand, Cut1p is thought to be a component, regulator, or motor for the spindle pole body or kinetochores (Uzawa *et al.*, 1990). Further work on *ptr4*, including cloning of the *ptr4*$^+$ gene, is now in progress to elucidate its functions in mRNA transport.

Pre-mRNA Splicing in the ptr Mutants

Northern blot analysis of TFIID mRNA suggests that only *ptr2/pim1* has defects in pre-mRNA splicing at the nonpermissive temperature. The other three isolated transport mutants showed no defects in pre-mRNA splicing. We examined defects of poly(A)$^+$ RNA transport in the *S. pombe* pre-mRNA splicing mutants (*prp1-13*) and found that only *prp1* was defective in poly(A)$^+$ RNA transport (Urushiyama *et al.*, 1996). Therefore, it appears that there is no general coupling between pre-mRNA splicing and nucleocytoplasmic transport of mRNA.

No oversized transcripts were detected in *ptr2/pim1* as in *mtr1/prp20*, which is a counterpart of *ptr2/pim1* in *S. cerevisiae*. Curiously, *mtr1–1* was reported to have no defects in splicing of *CRY1* pre-mRNA, although it is allelic with one of the well-known pre-mRNA splicing mutations, *prp20* (Kadowaki *et al.*, 1993). Thus, inhibition of the pre-mRNA splicing in *ptr2/pim1* and *mtr1/prp20* may be an allele-specific phenotype.

Ran GTPase Cycle and mRNA Export

The *ptr2*$^+$ gene was found to be identical to the *pim1*$^+$ gene, which encodes the *S. pombe* homologue of mammalian RCC1. It was known that *pim1* has defects in the poly(A)$^+$ RNA export (Kadowaki *et al.*, 1993; Tani *et al.*, 1995). The RCC1 protein in mammalian cells functions as a nuclear guanine nucleotide exchange factor for the guanosine triphosphatase Ran/TC4. A mutation or depletion of RCC1 in mammalian cells has pleiotropic effects (Sazer, 1996), including suppression of nuclear protein import (Tachibana *et al.*, 1994). Our result suggesting that the *ptr2* mutation has a temperature-sensitive defect in the nuclear import of the nucleoplasmin-GFP fusion is consistent with this previous report. A mutation in the *MTR1/PRP20/SRM1* gene encoding an RCC1 homologue in *S. cerevisiae* blocks mRNA export (Kadowaki *et al.*, 1993). A mutation within the GTPase-activating enzyme, an antagonistic regulator to RCC1, also blocks the mRNA export in *S. cerevisiae* (Schneiter *et al.*, 1995). These results suggest that the Ran GTPase system plays an important role in the transport of mRNA and protein. It may be that the mRNA transport pathway is one of the primary targets of the Ran-GTPase system as suggested (Sazer 1996). One cannot conclude, however, that the inhibition of mRNA transport is a direct consequence of perturbation of the Ran-GTPase cycle, since the Ran-GTPase system affects various cellular processes including RNA metabolism, cell cycle progression, and protein transport (for review, see Sazer, 1996).

Ubiquitin-activating Enzyme E1 Is Involved in mRNA Transport

We have shown that the *ptr3*$^+$ gene encodes a homologue of the ubiquitin-activating enzyme E1 in *S. pombe*. Ubiquitin-activating enzyme E1 is involved in the initial and essential step of the ubiquitin conjugation. Ubiquitin, a highly conserved protein with 76 amino acid residues, is covalently conjugated to other proteins and functions as a tag for ATP-dependent degradation of certain proteins (for review, see Jentsch *et al.*, 1991). Ubiquitin-dependent proteolysis is involved in both the selective elimination of abnormal proteins and the down-regulation of short-lived proteins such as crucial cellular regulators. However, it has become evident that ubiquitin may not function as a simple degradation tag, since many metabolically stable ubiquitin conjugates have been identified. The ubiquitin conjugation mediates diverse cellular functions such as cell cycle control, DNA repair, ribosome biogenesis, and stress response as well as protein degradation (Jentsch *et al.*, 1991).

This article appears to be the first report suggesting that the functional ubiquitin-activating enzyme E1 is related to the poly(A)$^+$ RNA export from the nucleus and to nuclear protein import. Blockage of mRNA export or protein import in *ptr3* may be one of the primary consequences of the mutation in ubiquitin-activating enzyme E1, as this enzyme has pleiotropic effects on many cellular events. One possible explanation for the involvement of ubiquitin-activating enzyme E1 in mRNA transport is that it may modulate efficient release of transcripts from the transcription or processing sites by mediating degradation of proteins anchoring mRNAs or by alteration in a higher order chromatin structure required for mRNA release. Ubiquitination of chromosomal proteins may either modulate the chromatin structure directly or mediate the degradation of chromosomal proteins. Retention of the poly(A)$^+$ RNA in the chromatin-rich region in *ptr3* supports this notion. Alternatively, it is possible that the accumulation of poly(A)$^+$ RNA in the nuclei or block of protein import in *ptr3* is a secondary effect of the disturbance of ubiquitin-dependent cellular processes such as cell cycle progression. Further investi-

gation of these mutants will be necessary to elucidate the exact roles of Ptr proteins in the mRNA export and protein import.

ACKNOWLEDGMENTS

We thank T. Matsumoto for providing the *S. pombe* genomic library, K. Kohno for GFP-nucleoplasmin plasmid pCHR5ST, and Y. Jin and H.R. Horvitz for the GFP-TT version of plasmid. We also thank K. Ogura and other members of our laboratory for discussion and M. Ohara for language assistance. This research was supported by grants from the Ministry of Education, Science, Sports and Culture of Japan.

REFERENCES

Altschul, S.F., Gish, W., Miller, W., Myers, E.W., and Lipman, D.J. (1990). Basic local alignment search tool. J. Mol. Biol. *215*, 403–410.

Amberg, D.C., Goldstein, A., and Cole, C.N. (1992). Isolation and characterization of *RAT1*: an essential gene of *Saccharomyces cerevisiae* required for the efficient nucleocytoplasmic trafficking of mRNA. Gene Dev. *6*, 1173–1189.

Aris, J.P., and Blobel, G. (1988). Identification and characterization of a yeast nucleolar protein that is similar to a rat liver nucleolar protein. J. Cell Biol. *107*, 17–31.

Bischoff, F.R., Krebber, H., Kempf, T., Hermes, I., and Ponstingl, H. (1995). Human RanGTPase-activating protein RanGAP1 is a homologue of yeast Rna1p involved in mRNA processing and transport. Proc. Natl. Acad. Sci. USA *92*, 1749–1753.

Bossie, M.A., DeHoratius, Barcelo, C., G., and Silver, P. (1992). A mutant nuclear protein with similarity to RNA binding proteins interferes with nuclear import in yeast. Mol. Biol. Cell *3*, 875–893.

Brown, J.A., Bharathi, A., Ghosh, A., Whalen, W., Fitzgerald, E., and Dhar, R. (1995). A mutation in the *Schizosaccharomyces pombe rae1* gene causes defects in poly(A)$^+$ RNA export and in the cytoskeleton. J. Biol. Chem. *270*, 7411–7419.

Chalfie, M., Tu, Y., Euskirchen, G., Ward, W.W., and Prasher, D.C. (1994). Green fluorescent protein as a marker for gene expression. Science *263*, 802–805.

Cottarel, G., Beach, D., and Deuschle, U. (1993). Two new multipurpose multicopy *Schizosaccharomyces pombe* shuttle vectors, pSP1 and pSP2. Curr. Genet. *23*, 547–548.

Dohmen, R.J., Stappen, R., McGrath, J.P., Forrova, H., Kolarov, J., Gotteau, A., and Varshavsky, A. (1995). An essential yeast gene encoding a homolog of ubiquitin-activating enzyme. J. Biol. Chem., *270*, 18099–18109.

Earnshaw, W.C., Halligan, B., Cooke, C.A., Heck, M.M.S., and Liu, L.F. (1985). Topoisomerase II is a structural component of mitotic chromosome scaffolds. J. Cell Biol. *100*, 1706–1715.

Eckner, R., Ellmeier, W., and Birnstiel, M.L. (1991). Mature mRNA 3′ end formation stimulates RNA export from the nucleus. EMBO J. *10*, 3513–3522.

Fischer, U., Huber, J., Boelens, W.C., Mattaj, I.W., and Lührmann, R. (1995). The HIV-1 Rev activation domain is a nuclear export signal that accesses an export pathway used by specific cellular RNAs. Cell *82*, 475–483.

Forrester, W., Stutz, F., Rosbash, M., and Wickens, M. (1992). Defects in mRNA 3′-end formation, transcription initiation, and mRNA transport associated with the yeast mutation *prp20*: possible coupling of mRNA processing and chromatin structure. Genes Dev. *6*, 1914–1926.

French, B.T., Schumm, D.E., and Webb, T.E. (1987). Active transport of messenger ribonucleoprotein particle in a reconstituted cell-free system. Proc. Natl. Acad. Sci. USA *84*, 5163–5166.

Gorsch, L.C., Dockendorff, T.C., and Cole, C.N. (1995). A conditional allele of the novel repeat-containing yeast nucleoporin *RAT7/NUP159* causes both rapid cessation of mRNA export and reversible clustering of nuclear pore complexes. J. Cell Biol. *129*, 939–955.

Guthrie, C., and Fink, G.R (1991). Guide to yeast genetics and molecular biology. Methods Enzymol. *194*, 795–823.

Hamm, J., and Mattaj, I.W. (1990). Monomethylated cap structures facilitate RNA export from the nucleus. Cell *63*, 109–118.

Heath, C.V., Copeland, C.S., Amberg, D.C., Priore, V.D., Snyder, M., and Cole, C.N. (1995). Nuclear pore complex clustering and nuclear accumulation of poly(A)$^+$ RNA associated with mutation of the *Saccharomyces cerevisiae RAT2/NUP120* gene. J. Cell Biol. *131*, 1677-1697.

Hirano, T., Funahashi, S., Uemura, T., and Yanagida, M. (1986). Isolation and characterization of *Schizosaccharomyces pombe cut* mutants that block nuclear division but not cytokinesis. EMBO J. *11*, 2973–2979.

Huang, Y., and Carmichael, G.G. (1996). Role of polyadenylation in nucleocytoplasmic transport of mRNA. Mol. Cell. Biol. *16*, 1534–1542.

Jarmolowski, A., Boelens, W.C., Izaurralde, E., and Mattaj, I.W. (1994). Nuclear export of different classes of RNA is mediated by specific factors. J. Cell Biol. *124*, 627–635.

Jentsch, S., Seufert, W., and Hauser, H.-P., (1991). Genetic analysis of the ubiquitin system. Biochim. Biophys. Acta *1089*, 127–139.

Kadowaki, T., Goldfarb, D., Spitz, L.M., Tartakoff, A.M., and Ohno, M. (1993). Regulation of RNA processing and transport by a nuclear guanine nucleotide release protein and members of the Ras superfamily. EMBO J. *12*, 2929–2937.

Kadowaki, T., Chen, S., Hitomi, M., Jacobs, E., Kumagai, C., Liang, S., Schneiter, R., Singleton, D., Wisniewska, J., and Tartakoff, A.M. (1994a). Isolation and characterization of *Saccharomyces cerevisiae* mRNA transport-defective (*mtr*) mutants. J. Cell Biol. *126*, 649–659.

Kadowaki, T., Hitomi, M., Chen, S., and Tartakoff, A.M. (1994b). Nuclear mRNA accumulation causes nucleolar fragmentation in yeast *mtr2* mutant. Mol. Biol. Cell *5*, 1253–1263.

Li, O., Heath, C.V., Amberg, D.C., Dockendorff, T.C., Copeland, C.S., Snyder, M., and Cole, C.N. (1995). Mutation or deletion of the *Saccharomyces cerevisiae RAT3/NUP133* gene causes temperature dependent nuclear accumulation of poly(A)$^+$ RNA and constitutive clustering of nuclear pore complexes. Mol. Biol. Cell *6*, 401–417.

Lim, C.R., Kimata, Y., Oka, M., Nomaguchi, K., and Kohno K. (1995). Thermosensitivity of green fluorescent protein fluorescence utilized to reveal nuclear-like compartments in a mutant nucleoporin NSP1. J. Biochem. *118*, 13–17.

Matsumoto, T., and Beach, D. (1991). Premature initiation of mitosis in yeast lacking RCC1 or an interacting GTPase. Cell *66*, 347–360.

Maundrell, K. (1993). Thiamine -repressible expression vectors pREP and pRIP for fission yeast. Gene *123*, 127–130.

McGrath, J.P., Jentsch, S., and Varshavsky, A. (1991). UBA1: an essential yeast gene encoding ubiquitin-activating enzyme. EMBO J. *10*, 227–236.

Michael, W.M., Choi, M., and Dreyfuss, G. (1995). A nuclear export signal in hnRNP A1: a signal-mediated, temperature-dependent nuclear protein export pathway. Cell *83*, 415–422.

Moffet, R.B., and Webb, T.E. (1981). Regulated transport of messenger ribonucleic acid from isolated liver nuclei by nucleic acid binding proteins. Biochemistry *20*, 3253–3262.

Nigg, E.A., Baeuerle, P.A., and Lührmann, R. (1991). Nuclear import-export: in search of signals and mechanisms. Cell *66*, 15–22.

Nischt, R., Thüroff, E., and Käufer, N.F., (1986). Molecular cloning of a ribosomal gene from the fission yeast *Schizosaccharomyces pombe*. Curr. Genet. *10*, 365–370.

Okazaki, K., Okazaki, N., Jinno, S., Tanaka, K., and Okayama, H. (1990). High-frequency transformation and library transducing vectors for cloning mammalian cDNAs by trans-complementation of *Schizosaccharomyces pombe*. Nucleic Acids Res. *18*, 6485–6489.

Piñol-Roma, S., and Dreyfuss, G. (1991). Transcription-dependent and transcription-independent nuclear transport of hnRNP proteins. Science *253*, 312–314.

Piñol-Roma, S., and Dreyfuss, G. (1992). Shuttling of pre-mRNA binding proteins between nucleus and cytoplasm. Nature *355*, 730–732.

Riedel, N., and Fasold, H. (1992). Role of mRNA transport in post-transcriptional control of gene expression. In: Nuclear Trafficking, ed. C.M. Feldherr, London: Academic Press, 231–290.

Sambrook, J., Fritsch, E.F., and Maniatis, T. (1989). Molecular Cloning: A Laboratory Manual, 2nd ed., Cold Spring Harbor, NY: Cold Spring Harbor Laboratory Press.

Santiago, T.C., Purvis, I.J., Bettany, A.J. E., and Brown, A.J. P. (1986). The relationship between mRNA stability and length in *Saccharomyces cerevisiae*. Nucleic Acids Res. *14*, 8347–8360.

Sazer, S. (1996). The search for the primary function of the Ran GTPase continues. Trends Cell Biol. *6*, 81–85.

Schneiter, R., Kadowaki, T., and Tartakoff, A.M. (1995). mRNA transport in yeast: time to reinvestigate the function of the nucleolus. Mol. Biol. Cell *6*, 357–370.

Schröder, H.C., Friese, U., Bachmann, M., Zaubitzer, T., and Müller, W.E. G. (1989). Energy requirement and kinetics of transport of poly(A)-free histone mRNA compared to poly(A)-rich mRNA from isolated L-cell nuclei. Eur. J. Biochem. *181*, 149–158.

Shiokawa, K., and Pogo, A.O. (1974). The role of cytoplasmic membrane in controlling the transport of nuclear messenger RNA and initiation of protein synthesis. Proc. Natl. Acad. Sci. USA *71*, 2658–2662.

Singleton D.R., Chen, S., Hitomi, M., Kumagai, C., and Tartakoff, A.M. (1995). A yeast protein that bidirectionally affects nucleocytoplasmic transport. J. Cell Sci. *108*, 265–272.

Tachibana, T., Imamoto, N., Seino, H., Nishimoto, T., and Yoneda, H. (1994). Loss of RCC1 leads to suppression of nuclear protein import in living cells. J. Biol. Chem. *269*, 24542–24545.

Tani, T., Derby, R.J., Hiraoka, Y., and Spector, D.L. (1995). Nucleolar accumulation of poly(A)$^+$ RNA in heat-shocked yeast cells: implication of nucleolar involvement in mRNA transport. Mol. Biol. Cell *6*, 1515–1534.

Uemura, T., and Yanagida, M. (1984). Isolation of type I and II DNA topoisomerase mutants from fission yeast: single and double mutants show different phenotypes in cell growth and chromatin organization. EMBO J. *3*, 1737–1744.

Uemura, T., and Yanagida, M. (1986). Mitotic spindle pulls but fails to separate chromosomes in type II DNA topoisomerase mutants: uncoordinated mitosis. EMBO J. *5*, 1003–1010.

Urushiyama, S., Tani, T., and Ohshima, Y. (1996). Isolation of novel pre-mRNA splicing mutants of *Schizosaccharomyces pombe*. Mol. Gen. Genet. *253*, 118–127.

Uzawa, S., Samejima, I., Hirano, T., Tanaka, K., and Yanagida, M. (1990). The fission yeast *cut1* $^+$ gene regulates spindle pole body duplication and has homology to the budding yeast *ESP1* gene. Cell *62*, 913–925.

Vijayraghavan, U., Company, M., and Abelson, J. (1989). Isolation and characterization of pre-mRNA splicing mutants of *Saccharomyces cerevisiae*. Genes Dev. *3*, 1206–1216.

Zacksenhaus, E., and Sheinin, R. (1990). Molecular cloning, primary structure and expression of the human X linked A1S9 gene cDNA which complements the tsA1S9 mouse L cell defect in DNA replication. EMBO J. *9*, 2923–2929.